

Photoinduced β -fragmentation of aliphatic alcohol derivatives for forging C–C bonds

Received: 8 August 2022

Accepted: 22 November 2022

Published online: 02 December 2022

Check for updates

Yiman Gao¹, Jie Liu¹, Cong Wei¹, Yan Li¹, Kui Zhang¹, Liangliang Song¹ & Lingchao Cai¹✉

Alcohols are ubiquitous in chemistry and are native functionalities in many natural products and bioactive molecules. As such, a strategy that utilizes hydroxy-containing compounds to develop bond disconnection and bond formation process would achieve molecular diversity. Herein we utilize bench-stable *N*-alkoxyphthalimides prepared from alcohols to couple with glycine derivatives via radical process under visible light irradiation, providing a variety of unnatural amino acid (UAA) and peptide derivatives. The approach allows to rapidly deconstruct molecular complexity via β -fragmentation such as saclareolide, β -pinene and camphor and provides products with unique scaffolds, which show inhibition toward the pathogenic fungi growth.

Around 50 of 2021s top-200 best-selling small molecule pharmaceuticals contain α -amino acid-derived scaffolds as exemplified by lenalidomide, lisdexamfetamine, lacosamide, carfilzomib, and brivaracetam (Fig. 1a)¹. Meanwhile, UAAs have been genetically encoded in various cells and model organisms, investigating the structure and dynamics of proteins, to study their interactions and functions, to control their activities in living cells, as well as to introduce novel functions in proteins unachievable in nature². As such, amino acids are valuable and indispensable building blocks in the manufacture of a wide range of pharmaceuticals and biological applications.

Aliphatic alcohols are found ubiquitously in pharmaceuticals, agricultural chemicals, biomass degradation products, and many bioactive natural products (Fig. 1b). Classically, the Grignard reaction is an often adopted method for utilization of alcohols with an addition toward carbonyl-derived substrates, which is a prominent textbook process to form new C–C bonds and widely applied in synthetic and pharmaceutical chemistry for complex natural product syntheses^{3–6} and drug development^{7,8} since its discovery in 1912 (Fig. 1c)^{9–12}. The conversion toward Grignard reagents from alcohols typically requires two-step procedures: Appel reaction and magnesium metal reduction. From a safety perspective, the preparation of Grignard reagents with magnesium metal is often hard to control, and strongly exothermic as the subsequent Grignard addition. Meanwhile, Grignard reaction suffer from low functional group tolerance and hazardous wastes. Furthermore, the bond formation becomes less efficient when steric

hindrance is amplified, limiting its broad utility. Given the potential applications of Grignard-type reactions, especially in complex molecule syntheses and the importance of UAAs, the development of a convenient protocol for C–C bond formation from ubiquitous alcohol precursors under mild conditions is an enduring demand and fulfills the requirement of chemical sustainability.

Recently, radical approaches for selective functional transformations under photocatalyzed conditions experience a surge of developments, which switch the traditional two-electron approach to a single-electron approach, thus achieving various challenging transformations, which are unattainable by classical methods. The photo-induced alkoxy radical has emerged as a versatile intermediate and has been applied in a wide variety of synthetic transformations^{13–15}. Proton-coupled electron transfer (PCET)^{16,17}, ligand-to-metal charge transfer (LMCT)^{18–23}, transition metal mediated homolysis^{24–31}, and in situ generation of O–X species^{32,33}, have appeared as powerful strategies to enable the alkoxy radical-based hydrogen atom transfer³⁴, β -fragmentation³⁵, and alkene addition³⁶. Meanwhile, alkoxy radical generation from *N*-alkoxyphthalimides triggered by a transient reductant that is generated by low-intensity irradiation with visible light is used preferred as alternative^{37–41}, among many other oxygen-heteroatom bonds precursors such as nitrites⁴², nitrates⁴³, hypohalites⁴⁴, and sulphenates⁴⁵, etc. due to its stability and accessibility. Chen³⁷, Tang³⁸, Aggarwal^{39,41}, and Martin⁴⁰ groups, respectively, developed attractive methodologies to achieve C(sp³)-C(sp³),

¹Jiangsu Co-Innovation Center of Efficient Processing and Utilization of Forest Resources, International Innovation Center for Forest Chemicals and Materials, Jiangsu Province Key Laboratory of Green Biomass Based Fuels and Chemicals, College of Chemical Engineering, Nanjing Forestry University, Nanjing 210037, China. ✉ e-mail: cailingchao@njfu.edu.cn

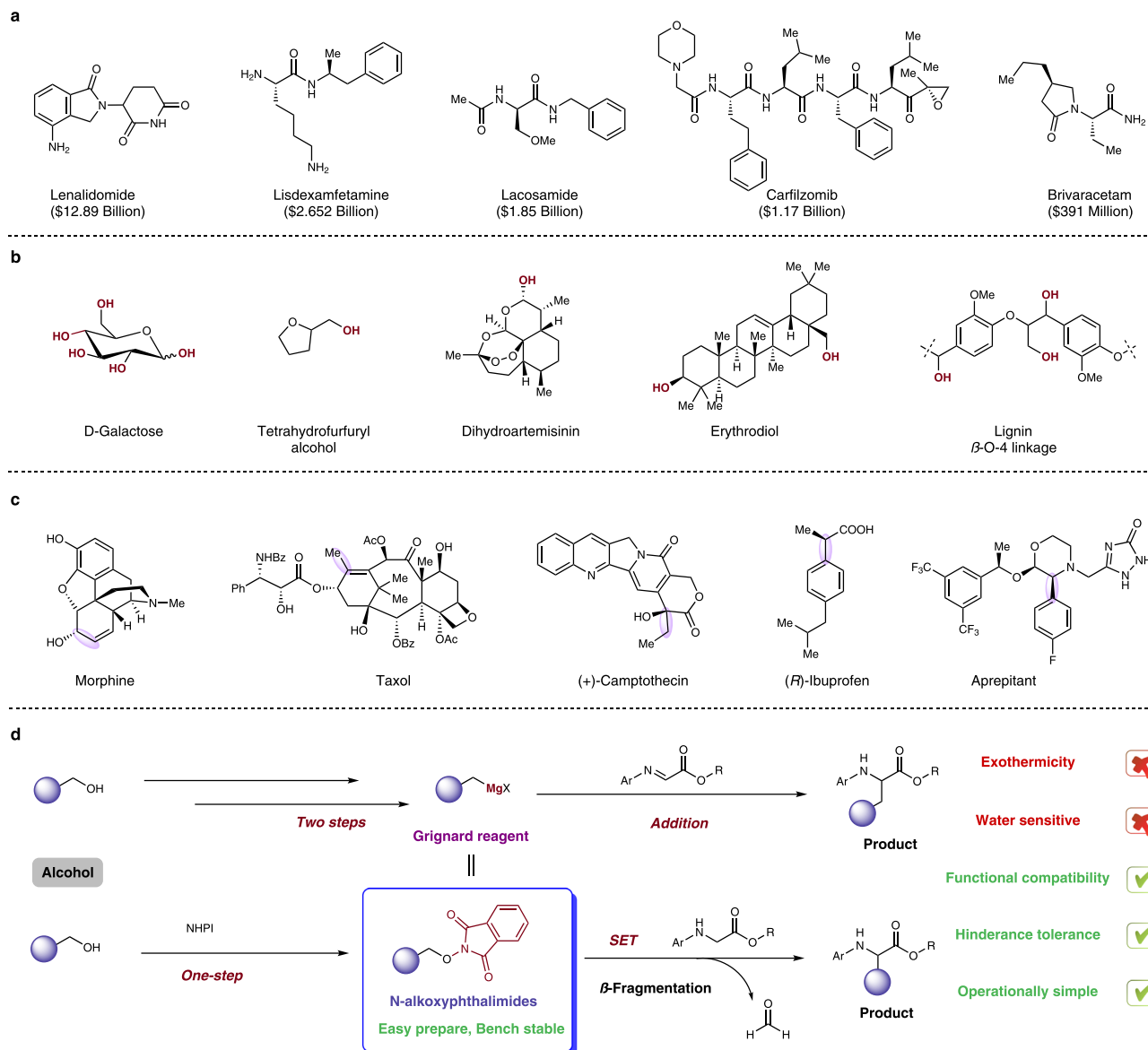


Fig. 1 | Project background and design plan. **a** Various drugs derived from α -amino acid; **b** Representative biomass derivatives, pharmaceuticals, and natural products containing hydroxy functional group; **c** Pharmaceutical and natural products syntheses featuring the Grignard reaction (formed bonds highlighted in

purple); **d** Classical Grignard transformation from alcohols and our *N*-alkoxyphthalimide-based alternative approach. NHPI, *N*-hydroxyphthalimide, SET single-electron transfer.

$C(\text{sp}^3)\text{-B}$, and $C(\text{sp}^3)\text{-C}(\text{sp}^2)$ bond formation from *N*-alkoxyphthalimides (NHPI) precursors via alkoxy radical.

Herein, we devised a strategy between bench stable *N*-alkoxyphthalimides prepared from alcohols and glycine derivatives to form C–C bonds via a redox-neutral radical–radical coupling process as alternative to Grignard-type addition, bypassing the need to utilize harsh organometallic reagents and minimizing the adverse environmental impact (Fig. 1d).

Results

Reaction optimization

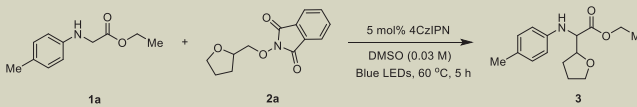
We started our model reaction using ethyl *p*-tolylglycinate (**1a**) and tetrahydrofurfuryl alcohol-derived *N*-alkoxyphthalimide **2a** (Table 1). Gratifyingly, the desired product **3** was isolated in 92% (d.r. = 1:1) when the reaction was carried out in DMSO at 60 °C for 5 h with blue LED irradiation and 4CzIPN as a photocatalyst (Table 1, entry 1). Other photocatalysts such as TTP, eosin Y, Acr⁺-Mes, and rhodamine B were proved ineffective for this transformation (Table 1, entries 2–5). 60 °C

and DMSO were proved to be the optimal temperature and solvent for this reaction (Table 1, entries 6–9). During the optimization process, we found higher reaction concentration would diminish the reaction efficiency and the 0.03 M gave the best result (Table 1, entry 10). Control experiments also demonstrated that the reaction could not occur in the absence of either the photocatalyst or light (Table 1, entries 11–12).

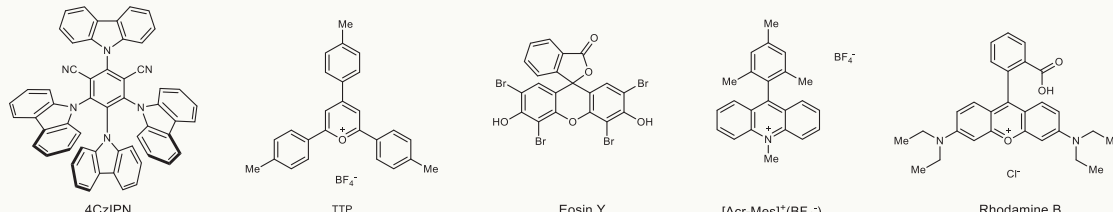
Evaluation of substrate scopes

Having established the optimal reaction conditions, we proceeded to probe the scope of this transformation. We first evaluated this method with different *N*-alkoxyphthalimides. As shown in Fig. 2, various five and six-membered cyclic *N*-alkoxyphthalimides smoothly proceeded this transformation to provide the desired products **3–6** in good to excellent yields (60–92%). Benzylic and heteroaryl benzylic *N*-alkoxyphthalimides were also examined and found to be good substrates, regardless of the substituent on the aromatic ring (**7–10**, 46–82%). Notably, azido and alkynyl groups were well tolerated in the reaction

Table 1 | Optimization of the reaction conditions



Entry	Variation from the standard conditions	Yield (%) ^a
1	None	92 ^b
2	TTP instead of 4CzIPN	<5
3	Eosin Y instead of 4CzIPN	<5
4	[Acr-Mes] ⁺ (BF ₄ ⁻) instead of 4CzIPN	<5
5	Rhodamine B instead of 4CzIPN	<5
6	80 °C instead of 60 °C	70
7	40 °C instead of 60 °C	69
8	DMA instead of DMSO	75
9	MeCN instead of DMSO	56
10	0.1 M instead of 0.03 M	56
11	No photocatalyst	nd
12	No light	nd



Standard conditions: 5 mol% 4CzIPN, 0.2 mmol **1a**, 0.1 mmol **2a**, DMSO (0.03 M), 15 W Blue LEDs, 60 °C, 5 h. DMSO dimethyl sulfoxide, DMA dimethylacetamide, MeCN acetonitrile, nd not detected.

^aIsolated yield.

^bd.r. = 1: 1.

(**11** and **12**, 85 and 65%), which provided an opportunity for further “click bioconjugation”. Benzylic substrates with an additional substituent on the benzyl position were also compatible with this transformation, thus delivering the corresponding UAAs **13** and **14** in 65 and 73% yields, respectively. In order to prove the efficiency of this transformation in consideration of the steric effect, varieties of sterically bulky substrates were tested and synthetically useful yields (31–63%) were obtained, which offered complementarity to Grignard-type addition (**15–20**). It is worthy to mention that these sterically bulky substrates were easily prepared from sterically less hindered primary alcohols. *N*-alkoxyphthalimides derived from hemiacetal and cyclic tertiary alcohol reacted smoothly under the standard conditions and afforded ring-opened formate and ketone tethered products (**21–24**), whose functionalities could not be compatible with Grignard-type reaction conditions. Allylic and propargylic radicals could be generated facily from corresponding precursors and furnished the desired products in 77 and 65% yield, respectively (**25** and **26**). To our disappointment, *N*-alkoxyphthalimides which could generate alkenyl radical, aldehyde tethered products, and radical intermediates via 5-*exo-trig* process, failed to give any products. In addition, more complex scaffolds derived from sclareolide, β -pinene, *D*-camphor, glucose, coumarin, and gemfibrozil precursors were screened and offered simplified products in moderate to high yields (**27–32**, 25–86%) (Fig. 3).

Further expansion of the substrate scope was focused on glycine derivatives (Fig. 4). In order to prove the steric tolerance of this transformation, **2b** was employed as the substrate. The ethyl esters of

glycine bearing both electron-donating and electron-withdrawing groups on the aromatic ring were well tolerated (**15**, **33–38**), resulting in 50–73% yields. In addition, the efficiency was maintained when *N*-mesityl glycine ester was used for the reaction (**39**, 55%). Then switching the ethyl ester to benzyl, *tert*-butyl, and phenyl esters, the desired products were obtained in moderate yields (**41–43**, 38–55%). Glycerinamides and glycinitrile worked smoothly to deliver the desired products in 53–88% yields (**46–49**). *N*-aryl tetrahydroisoquinolines were employed for this reaction and gave coupling products in 51–56% yields (**50** and **51**). Substrates derived from natural products such as estrone, cholesterol, and menthol were successfully tolerated under standard conditions, reflecting the mildness of the reaction conditions (**52–54**). Finally, we found *N*-pyridine derived glycine ester worked for this reaction (**55**, 30%), giving promise for further exploring its application in agrochemical discovery.

Further utility of this transformation was demonstrated by conjugation of the peptide with **2b** (Fig. 5). The *N*-phenyl modified dipeptides, synthesized from a combination of glycine with alanine, glycine, phenylalanine, and tryptophan, successfully delivered the conjugated products in 51–68% yields (**56–59**). More complex tripeptide and tetrapeptide also demonstrated the efficiency of this transformation, furnishing the products in synthetically useful yields (**60** and **61**, 46% and 48%).

Examining functional group compatibility

After the demonstration of the broad substrate scope, especially coupling with the peptides, stimulated us to explore the compatibility

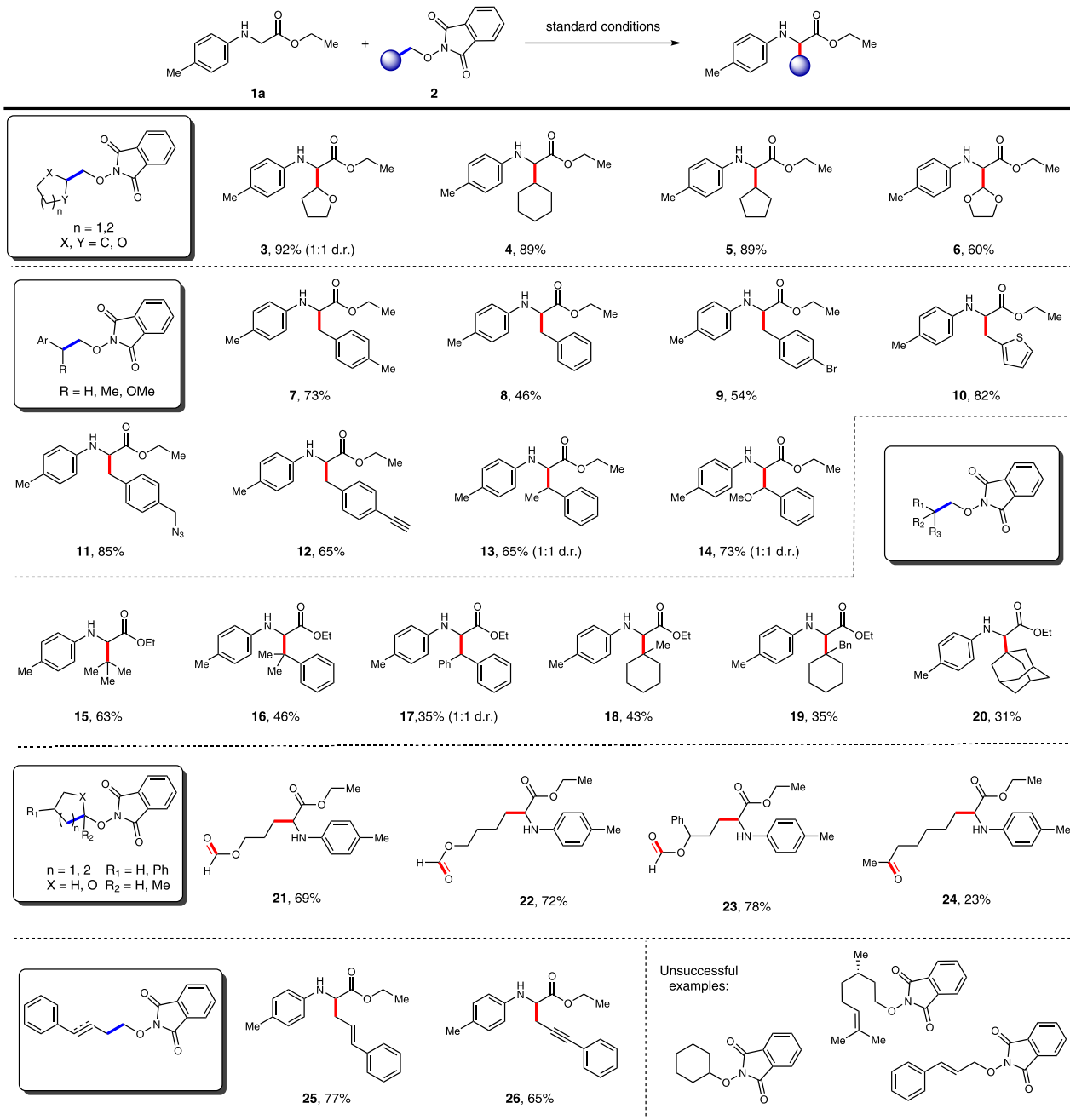


Fig. 2 | Scope of *N*-alkoxyphthalimides (broken bonds highlighted in blue and formed bonds highlighted in red). Conditions: All reactions were carried out with 4CzIPN (5 mol%), **1a** (0.2 mmol), **2** (0.1 mmol), and DMSO (0.03 M) irradiated under 15 W Blue LEDs at 60 °C.

with biomolecules, which could prove the possibility of this reaction for biological application. To this end, a mixture solvent system (H₂O: DMSO = 1: 4) and biological temperature (37 °C) was employed and a broad of biomolecules were selected, including nucleobase, amino acid, saccharide, biotin, protein, and DNA. As shown in Fig. 6, all reactions worked and gave desired product in the presence of these biomolecules (entries 1–9).

In vitro antifungal activities

Phytopathogenic fungi have imposed a major restriction on the stability and safety of agricultural production⁴⁶. Discovering novel antifungal agrochemicals from natural sources is highly appealing due to their low toxicity and easy degradation. Terpenes such as sclareolide, camphor, limonene, pinene, etc., have shown diverse biological

activities, including anti-bacteria, anti-fungus, and anti-tumor. By employing our decomplexity strategy, we transformed a few phytochemicals into glycine derivatives **27–29** with unique scaffolds and subjected these compounds against antifungal activity tests toward six crop pathogenic fungi with boscalid as a positive control. As shown in Table 2, (–)- β -pinene-derived compound **28** and (+)-camphor-derived compound **29** showed more potent activities than their parent compounds, respectively. However, compound **27** derived from sclareolide showed worse activities than sclareolide. Compound **29** presented fair to potent antifungal activities against *B. cinerea*, *S. sclerotiorum*, *C. orbiculare*, and *T. cucumeris*. The anti-*S. sclerotiorum* effect of compound **29** was up to 75%, which set a good starting point for further progress. In contrast, no inhibition was observed with camphor toward *S. sclerotiorum*. In addition, compound **29** showed

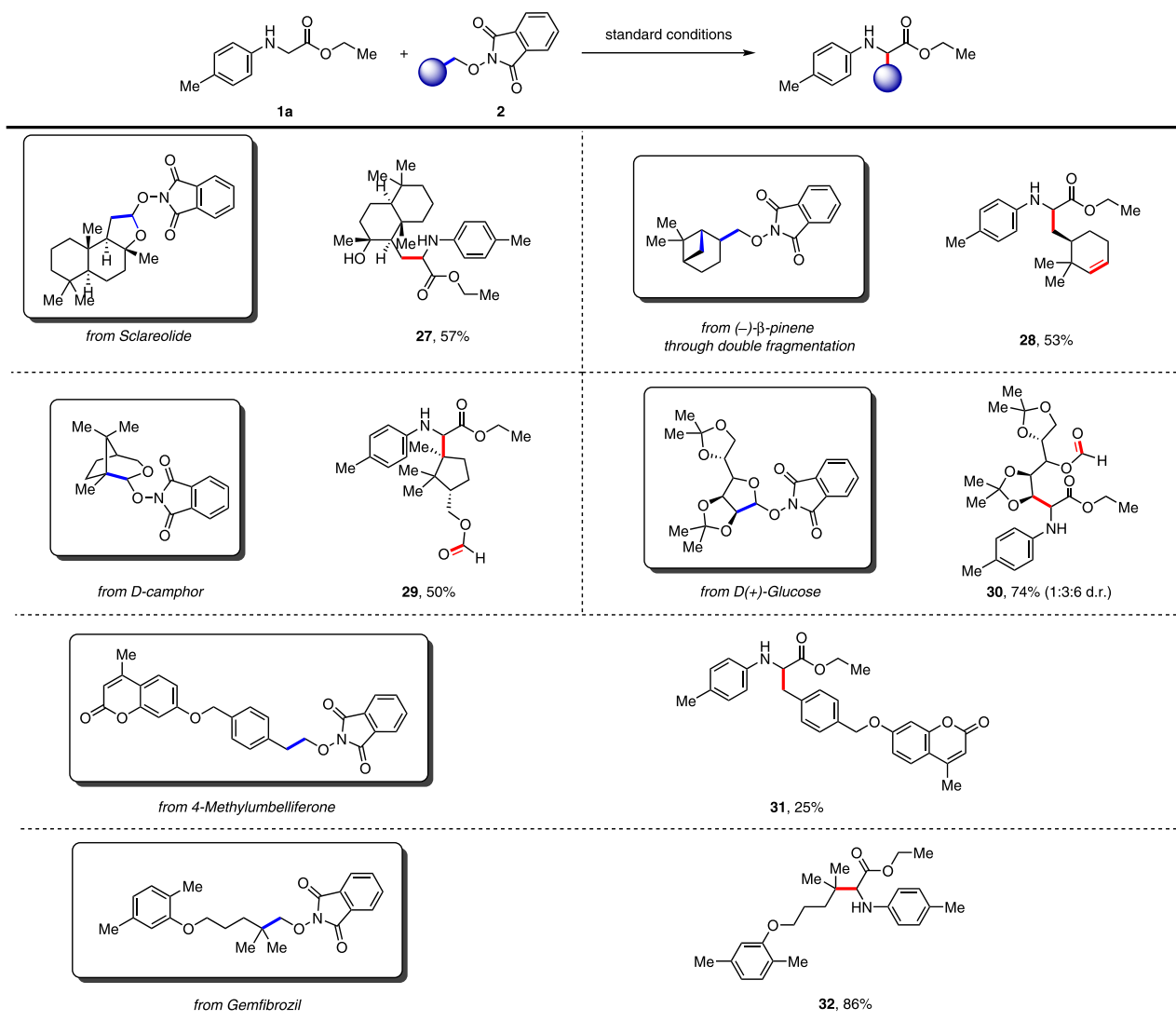


Fig. 3 | *N*-alkoxyphthalimides from nature sources. Conditions: All reactions were carried out with 4CzIPN (5 mol%), **1a** (0.2 mmol), **2** (0.1 mmol), and DMSO (0.03 M) irradiated under 15 W Blue LEDs at 60 °C.

better inhibition toward *C. orbiculare* and *C. paradoxa* than the positive control. The current preliminary anti-fungal activities indicate a promising prospect for further scaffold optimization based on terpenoid and glycine derivatives.

Mechanistic studies

To gain mechanistic insights into this coupling reaction, radical inhibitor 2,2,6,6-tetramethyl-1-piperidyloxy (TEMPO) was added to the model reaction system and it was found that it completely inhibited the coupling reaction (Fig. 7a eq.1). Moreover, during the substrate scope exploration, we could isolate the homo-coupling product in 12% yield (Fig. 7a eq.2). Furthermore, the radical clock was devised and ring-opened product **62** was isolated in 19% yield (Fig. 7a eq.3). Combining all the evidences from above reactions, a radical–radical coupling mechanism was proposed. As shown in Fig. 7b, the photoexcited 4CzIPN is able to undergo single-electron transfer (SET) reduction with *N*-alkoxyphthalimide substrates to form radical anion intermediate **I**, which could trigger the oxygen radical formation via phthalimide fragmentation. The resulting oxygen radical **II** quickly undergoes β -fragmentation to generate carbon-centered radical and radical stability explains the efficiency of *tert*-butyl radical addition. On the other way, glycine derivatives

could quench the oxidized 4CzIPN to regenerate the photocatalyst. Meanwhile, the resulting glycine radical could combine with carbon radical from *N*-alkoxyphthalimides to furnish the desired coupling products.

In conclusion, we have developed a convenient method based on a single-electron transfer process to construct C–C bond, which provides an alternative to the classical two-electron approach, bypassing the need to utilize harsh conditions and enabling the use of bench stable and easily prepared starting materials. The mild reaction conditions and broad functional group compatibility extend the application with peptides, making them preeminent and efficient species for potential biological and chemical applications. Deconstructing complex natural products offers a set of bioactive compounds and lays the foundation for further agrochemical development.

Methods

General procedure for the synthesis of 3–61

The *N*-alkoxyphthalimides (0.1 mmol), the esters, or amides of *N*-aryl-substituted glycine, or *N*-aryl tetrahydroisoquinoline, or peptides (0.2 mmol, 2.0 equiv.), 4CzIPN (5 mol%, 0.005 mmol, 4.0 mg), and DMSO (3 mL, 0.03 M) were added sequentially to a 4 mL clear-colored glass vial equipped with a magnetic stir bar. After bubbled with

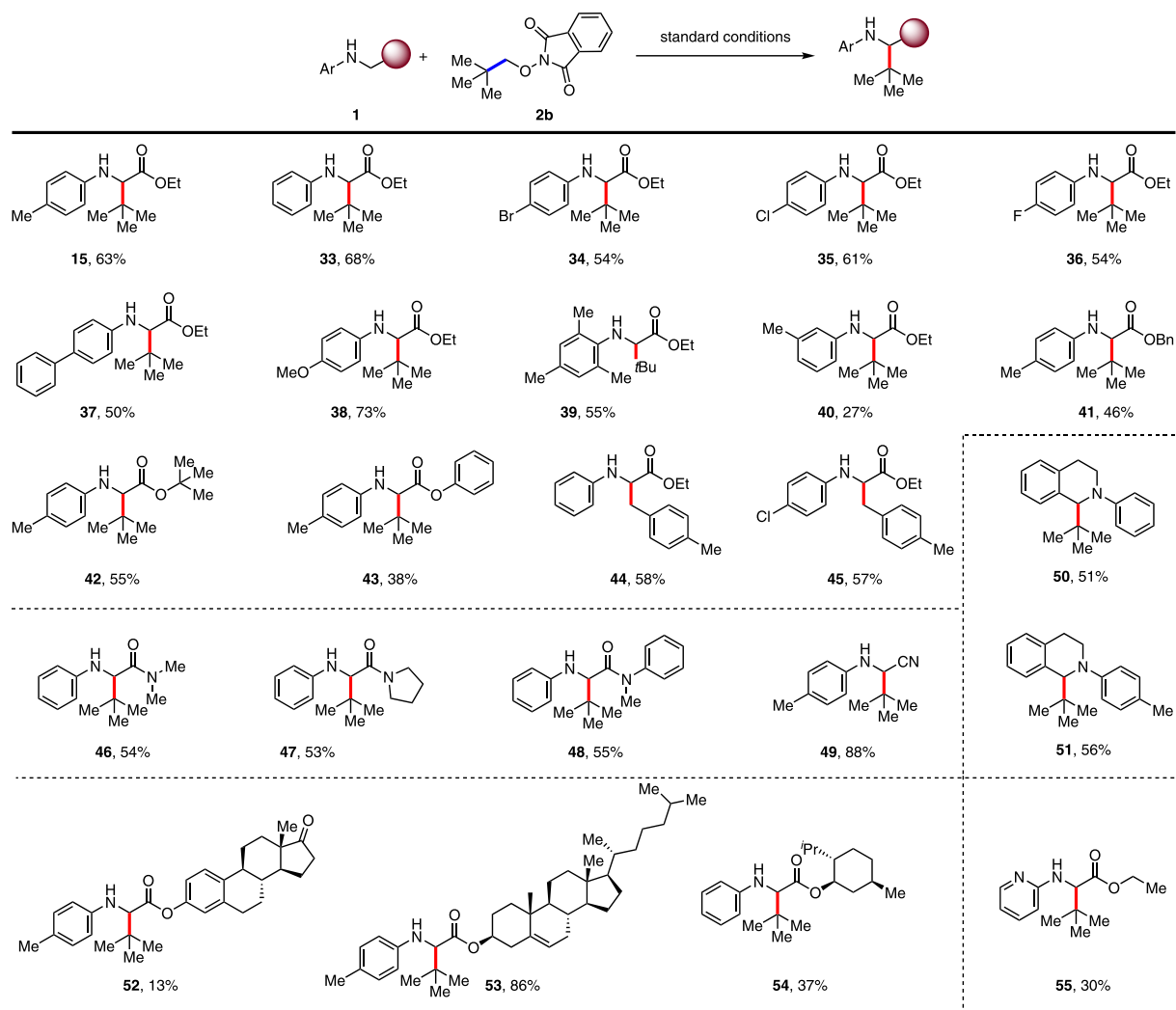


Fig. 4 | Scope of *N*-aryl protected derivatives. Conditions: All reactions were carried out with 4CzIPN (5 mol%), **1** (0.2 mmol), **2b** (0.1 mmol), and DMSO (0.03 M) irradiated under 15 W Blue LEDs at 60 °C.

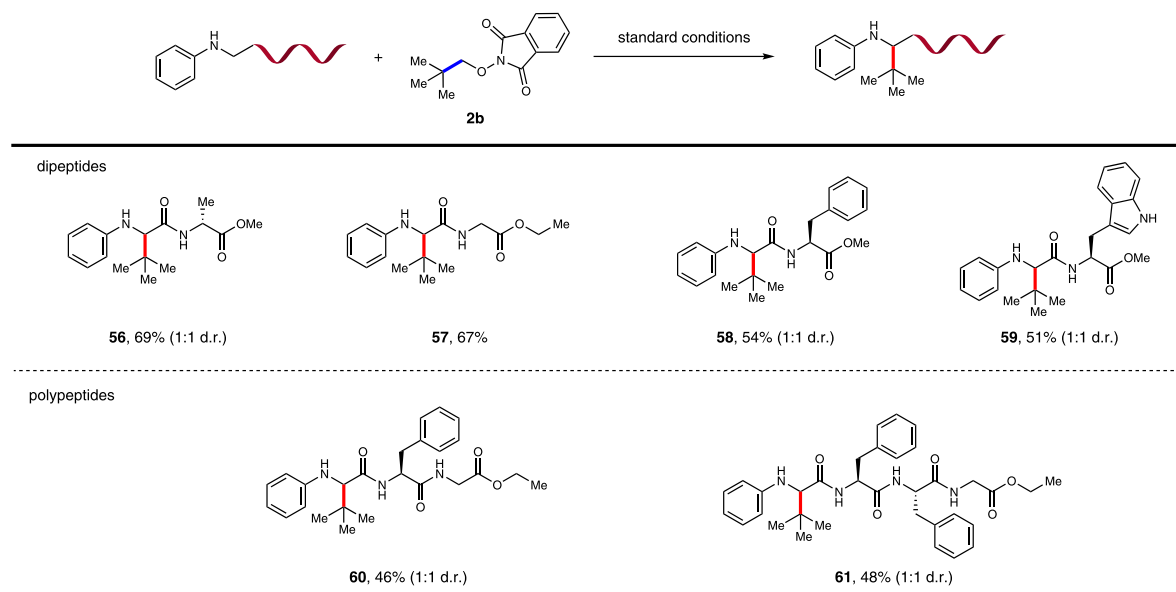


Fig. 5 | Scope of peptides. Conditions: All reactions were carried out with 4CzIPN (5 mol%), peptide (0.2 mmol), **2b** (0.1 mmol), and DMSO (0.03 M) irradiated under 15 W Blue LEDs at 60 °C.

nitrogen gas for 5 min to remove oxygen, the vial was sealed and exposed to blue LEDs at 60 °C. The reaction mixture was monitored by TLC until the starting material *N*-alkoxyphthalimides were consumed. Then, the reaction was quenched with water (2 mL), extracted with ethyl acetate, washed with brine, dried over anhydrous Na₂SO₄, concentrated in vacuo, and purified by column chromatography to yield the products **3–61**.

In vitro antifungal activities

Each target compound was dissolved in DMSO to prepare the stock solution (10.0 g/L). The stock solution was added to the PDA medium, and the concentration of target compounds in the medium was

50.0 mg/L. Pure DMSO without the target compounds was utilized as the blank control, and boscalid was coassayed as the reference compound. Fresh dishes with a diameter of 5 mm were taken from the edge

1a + 2b + Biomolecules $\xrightarrow[\text{Blue LEDs, 37 } ^\circ\text{C}]{\text{5 mol\% 4CzIPN, DMSO/H}_2\text{O (4/1)}}$ 15

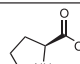
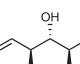
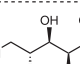
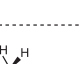
Entry	Biomolecules	Yield ^a	Entry	Biomolecules	Yield ^a
1	none	63%	6	 L-Proline (1 equiv.)	29%
2	Thymine (1 equiv.)	50%	7	 D-(-)-Ribose (1 equiv.)	86%
3	Adenine (1 equiv.)	77%	8	 D-(+)-Glucose (1 equiv.)	68%
4	10 mg ml ⁻¹ bovine serum albumin	32%	9	 D-Biotin (1 equiv.)	60%

Fig. 6 | Examining functional group compatibility. Conditions: All reactions were carried out with 4CzIPN (5 mol%), **1a** (0.2 mmol), **2b** (0.1 mmol), biomolecule, and DMSO (0.03 M) irradiated under 15 W Blue LEDs at 60 °C. ^a Yields were determined by HPLC analysis.

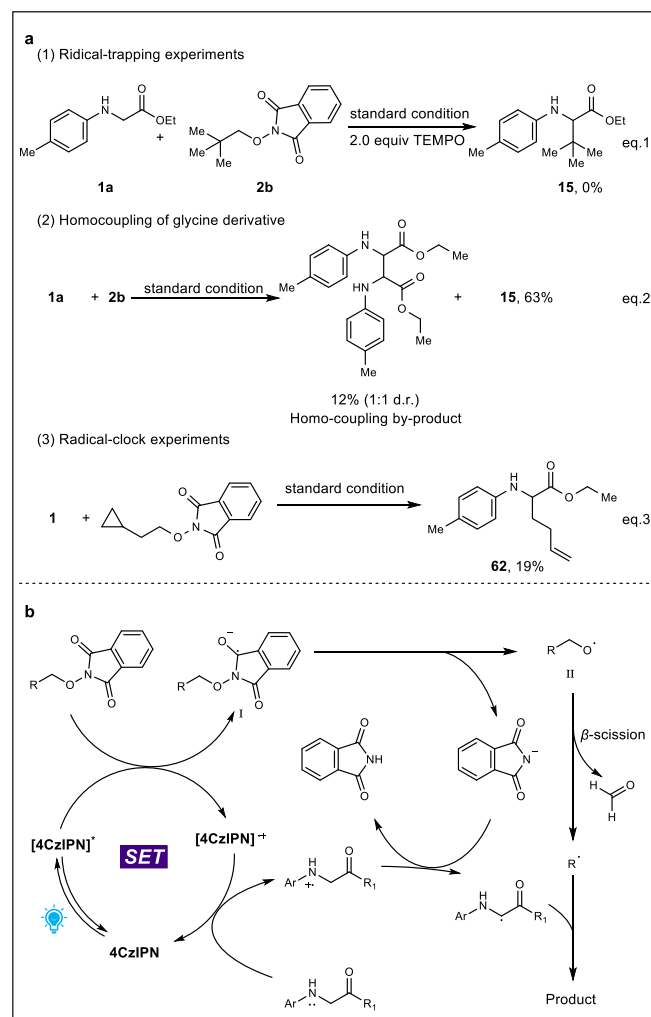
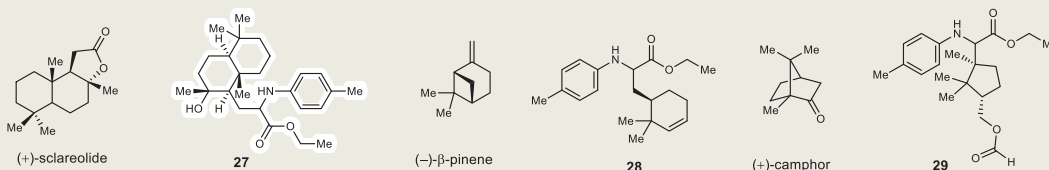


Fig. 7 | Mechanistic studies. a Control experiments; **b** Proposed mechanism.

Table 2 | In vitro antifungal activities of the target compounds at 50.0 mg/L

Compd	Inhibition rate (%) ^a					
	<i>B. cinerea</i>	<i>S. sclerotiorum</i>	<i>C. orbiculare</i>	<i>T. cucumeris</i>	<i>Alternariamali</i>	<i>C. paradoxa</i>
boscalid	90.3 ± 0.9	85.1 ± 0.8	21.5 ± 0.8	86.6 ± 1.5	82.5 ± 1.0	26.7 ± 3.8
(+)-sclareolide	16.7 ± 1.5	92.0 ± 1.9	23.9 ± 1.7	49.7 ± 2.6	40.4 ± 1.4	27.7 ± 4.5
27	2.7 ± 1.5	42.6 ± 3.3	5.4 ± 5.5	7.8 ± 2.4	7.7 ± 0.5	4.9 ± 1.3
(-)-β-pinene	—	52.7 ± 2.2	9.9 ± 0.4	5.9 ± 2.5	2.4 ± 1.3	9.1 ± 3.3
28	21.8 ± 3.9	40.1 ± 8.4	21.2 ± 1.0	44.4 ± 0.4	24.9 ± 2.9	26.2 ± 1.8
(+)-camphor	—	—	3.8 ± 1.7	18.7 ± 3.9	13.5 ± 1.3	27.9 ± 1.5
29	36.7 ± 1.9	75.0 ± 4.6	33.1 ± 1.7	45.7 ± 3.2	29.6 ± 1.3	29.9 ± 6.7



^a Values are the mean ± standard deviation of three replicates.

of the PDA-cultured fungi colonies and inoculated on the above three PDA media. Each treatment was tested for three replicates, and the antifungal effect was averaged. The relative inhibitory rate I (%) of all the tested compounds was calculated through the equation: I (%) = $[(C - T)/(C - 5)] \times 100$. In this equation, I is the inhibitory rate and C and T are the colony diameter of the blank control (mm) and treatment (mm), respectively.

Reporting summary

Further information on research design is available in the Nature Portfolio Reporting Summary linked to this article.

Data availability

The authors declare that all data supporting the findings of this study are available within the article and Supplementary Information files.

References

1. McGrath, N. A., Brichacek, M. & Njardarson, J. T. A graphical journey of innovative organic architectures that have improved our lives. *J. Chem. Educ.* **87**, 1348–1349 (2010).
2. Chin, J. W. Expanding and reprogramming the genetic code. *Nature* **550**, 53–60 (2017).
3. Chu, S., Münster, N., Balan, T. & Smith, M. D. A cascade strategy enables a total synthesis of (\pm)morphine. *Angew. Chem. Int. Ed.* **55**, 14306–14309 (2016).
4. Zhang, Q. et al. Enantioselective synthesis of *cis*-hydrobenzofurans bearing all-carbon quaternary stereocenters and application to total synthesis of (–)-morphine. *Nat. Commun.* **10**, 1–7 (2019).
5. Kanda, Y. et al. Two-phase synthesis of taxol. *J. Am. Chem. Soc.* **142**, 10526–10533 (2020).
6. Blagg, B. & Boger, D. Total synthesis of (+)-camptothecin. *Tetrahedron* **58**, 6343–6349 (2002).
7. Samineni, R., Eda, V., Rao, P., Sen, S. & Oruganti, S. Grignard reagents as niche bases in the synthesis of pharmaceutically relevant molecules. *ChemistrySelect* **7**, e202102853 (2022).
8. Kadam, A. et al. Comparative performance evaluation and systematic screening of solvents in a range of Grignard reactions. *Green. Chem.* **15**, 1880–1888 (2013).
9. Vollhardt, K. & Schore, N. *Organic Chemistry: Structure and Function* (W. H. Freeman, 2014).
10. Rappoport, Z. & Marek, I. (eds) *The Chemistry of Organomagnesium Compounds* (Wiley-VCH, 2008).
11. Seyferth, D. The Grignard reagents. *Organometallics* **28**, 1598–1605 (2009).
12. Doelstein, J. S. & Kozłowski, M. Organometal additions to α -iminoesters: N-alkylation via umpolung. *Chem. Soc. Rev.* **37**, 1166–1173 (2008).
13. Wu, X. & Zhu, C. Recent advances in alkoxy radical-promoted C-C and C-H bond functionalization starting from free alcohols. *Chem. Commun.* **55**, 9747–9756 (2019).
14. Tsui, E., Wang, H. & Knowles, R. R. Catalytic generation of alkoxy radicals from unfunctionalized alcohols. *Chem. Sci.* **11**, 11124–11141 (2020).
15. Chang, L., An, Q., Duan, L., Feng, K. & Zuo, Z. Alkoxy radicals see the light: new paradigms of photochemical synthesis. *Chem. Rev.* **122**, 2429–2486 (2022).
16. Miller, D. C., Tarantino, K. T. & Knowles, R. R. In *Hydrogen Transfer Reactions* (eds Guillena, G. & Ramón, D. J.) (Springer, 2016).
17. Gentry, E. C. & Knowles, R. R. Synthetic applications of proton-coupled electron transfer. *Acc. Chem. Res.* **49**, 1546–1556 (2016).
18. Yin, H., Carroll, P. J., Anna, J. M. & Schelter, E. J. Luminescent Ce(III) complexes as stoichiometric and catalytic photoreductants for halogen atom abstraction reactions. *J. Am. Chem. Soc.* **137**, 9234–9237 (2015).
19. Hu, A. et al. Cerium-catalyzed formal cycloaddition of cycloalkanols with alkenes through dual photoexcitation. *J. Am. Chem. Soc.* **140**, 13580–13585 (2018).
20. Hu, A. et al. δ -Selective functionalization of alkanols enabled by visible-light-induced ligand-to-metal charge transfer. *J. Am. Chem. Soc.* **140**, 1612–1616 (2018).
21. Hu, A., Guo, J. J., Pan, H. & Zuo, Z. Selective functionalization of methane, ethane, and higher alkanes by cerium photocatalysis. *Science* **361**, 668–672 (2018).
22. Zhang, K., Chang, L., An, Q., Wang, X. & Zuo, Z. Dehydroxymethylation of alcohols enabled by cerium photocatalysis. *J. Am. Chem. Soc.* **141**, 10556–10564 (2019).
23. Chen, Y., Du, J. & Zuo, Z. Selective C-C bond scission of ketones via visible-light-mediated cerium catalysis. *Chem* **6**, 266–279 (2020).
24. Zhao, H., Fan, X., Yu, J. & Zhu, C. Silver-catalyzed ring-opening strategy for the synthesis of β - and γ -fluorinated ketones. *J. Am. Chem. Soc.* **137**, 3490–3493 (2015).
25. Zhou, X. et al. Radical dehydroxymethylative fluorination of carbohydrates and divergent transformations of the resulting reverse glycosyl fluorides. *Angew. Chem. Int. Ed.* **59**, 4138–4144 (2020).
26. Ren, R., Zhao, H., Huan, L. & Zhu, C. Manganese-catalyzed oxidative azidation of cyclobutanols: regioselective synthesis of alkyl azides by C-C bond cleavage. *Angew. Chem. Int. Ed.* **54**, 12692–12696 (2015).
27. Ren, R., Wu, Z., Xu, Y. & Zhu, C. C-C bond-forming strategy by manganese-catalyzed oxidative ring-opening cyanation and ethynylation of cyclobutanol derivatives. *Angew. Chem. Int. Ed.* **55**, 2866–2869 (2016).
28. Zhu, Y. et al. Silver-catalyzed remote Csp³-H functionalization of aliphatic alcohols. *Nat. Commun.* **9**, 1–7 (2018).
29. Zhu, Y. et al. DMSO-Enabled selective radical O-H activation of 1,3(4)-diols. *Angew. Chem. Int. Ed.* **132**, 20023–20028 (2020).
30. Bovino, M. T. et al. Enantioselective copper-catalyzed carboetherification of unactivated alkenes. *Angew. Chem. Int. Ed.* **53**, 6383–6387 (2014).
31. Miller, Y., Miao, L., Hosseini, A. S. & Chemler, S. R. Copper-catalyzed intramolecular alkene carboetherification: synthesis of fused-ring and bridged-ring tetrahydrofurans. *J. Am. Chem. Soc.* **134**, 12149–12156 (2012).
32. Jia, K., Zhang, F., Huang, H. & Chen, Y. Visible-light-induced alkoxy radical generation enables selective C(sp³)-C(sp³) bond cleavage and functionalizations. *J. Am. Chem. Soc.* **138**, 1514–1517 (2016).
33. Jia, K., Pan, Y. & Chen, Y. Selective carbonyl-C(sp³) bond cleavage to construct ynamides, ynoates, and yrones by photoredox catalysis. *Angew. Chem. Int. Ed.* **56**, 2478–2481 (2017).
34. Guo, W., Wang, Q. & Zhu, J. Visible light photoredox-catalysed remote C-H functionalisation enabled by 1,5-hydrogen atom transfer (1,5-HAT). *Chem. Soc. Rev.* **50**, 7359–7377 (2021).
35. Murakami, M. & Ishida, N. β -Scission of alkoxy radicals in synthetic transformations. *Chem. Lett.* **46**, 1692–1700 (2017).
36. Hartung, J. Stereoselective construction of the tetrahydrofuran nucleus by alkoxy radical cyclizations. *Eur. J. Org. Chem.* **2001**, 619–632 (2001).
37. Zhang, J., Li, Y., Zhang, F., Hu, C. & Chen, Y. Generation of alkoxy radicals by photoredox catalysis enables selective C(sp³)-H functionalization under mild reaction conditions. *Angew. Chem. Int. Ed.* **55**, 1872–1875 (2016).
38. Han, J. Bin, Guo, A. & Tang, X. Y. Alkylation of allyl/alkenyl sulfones by deoxygenation of alkoxy radicals. *Chem. Eur. J.* **25**, 2989–2994 (2019).
39. Shu, C., Noble, A. & Aggarwal, V. K. Metal-free photoinduced C(sp³)-H borylation of alkanes. *Nature* **586**, 714–719 (2020).
40. Cong, F., Lv, X. Y., Day, C. S. & Martin, R. Dual catalytic strategy for forging sp²-sp³ and sp³-sp³ architectures via β -scission of aliphatic alcohol derivatives. *J. Am. Chem. Soc.* **142**, 20594–20599 (2020).

41. Shu, C., Madhavachary, R., Noble, A. & Aggarwal, V. K. Photo-induced fragmentation borylation of cyclic alcohols and hemiacetals. *Org. Lett.* **22**, 7213–7218 (2020).
42. Barton, D. H. R., Beaton, J. M., Geller, L. E. & Pechet, M. M. A new photochemical reaction. *J. Am. Chem. Soc.* **82**, 2640–2641 (1960).
43. Vite, G. D. & Fraser-Reid, B. Generation of oxygen-centered radicals by reaction of nitrate esters with tri-*n*-butyltin hydride. *Synth. Commun.* **18**, 1339–1342 (1988).
44. Walling, C. & Clark, R. T. Reactions of primary and secondary alkoxy radicals derived from hypochlorites. *J. Am. Chem. Soc.* **96**, 4530–4534 (1974).
45. Beckwith, A. L. J., Hay, B. P. & Williams, G. M. Generation of alkoxy radicals from O-alkyl benzenesulphenates. *J. Chem. Soc. Chem. Commun.* **17**, 1202–1203 (1989).
46. Sierotzki, H. & Scalliet, G. A review of current knowledge of resistance aspects for the next-generation succinate dehydrogenase inhibitor fungicides. *Phytopathology* **103**, 880–887 (2013).

Acknowledgements

This work was supported by the National Natural Science Foundation of China (22001136 to K.Z. and 22001124 to L.C.), Jiangsu Provincial Double-Innovation Doctor Program (JSSCBS20210555 to K.Z.), and the Jiangsu Specially-Appoint Professor Plan to L.C., the Natural Science Foundation of Jiangsu Province (BK20220409 to L.S.).

Author contributions

Y.G. and C.W. performed the synthetic experiments and analyzed the data. J.L. and Y.L. performed an antifungal activity test. K.Z., L.S., and L.C. designed and directed the project and wrote the manuscript.

Competing interests

K.Z., Y.G., J.L., L.C., and L.S. declare the following competing interests that one Chinese patent has been registered (202211194528.8). Y.L. declares no competing interest.

Additional information

Supplementary information The online version contains supplementary material available at <https://doi.org/10.1038/s41467-022-35249-7>.

Correspondence and requests for materials should be addressed to Lingchao Cai.

Peer review information *Nature Communications* thanks Guo-Qiang Xu, and the other, anonymous, reviewer for their contribution to the peer review of this work.

Reprints and permissions information is available at <http://www.nature.com/reprints>

Publisher's note Springer Nature remains neutral with regard to jurisdictional claims in published maps and institutional affiliations.

Open Access This article is licensed under a Creative Commons Attribution 4.0 International License, which permits use, sharing, adaptation, distribution and reproduction in any medium or format, as long as you give appropriate credit to the original author(s) and the source, provide a link to the Creative Commons license, and indicate if changes were made. The images or other third party material in this article are included in the article's Creative Commons license, unless indicated otherwise in a credit line to the material. If material is not included in the article's Creative Commons license and your intended use is not permitted by statutory regulation or exceeds the permitted use, you will need to obtain permission directly from the copyright holder. To view a copy of this license, visit <http://creativecommons.org/licenses/by/4.0/>.

© The Author(s) 2022